Oral Diseases (2008) 14, 713–726. doi:10.1111/j.1601-0825.2008.01489.x

http://www.blackwellmunksgaard.com

ORIGINAL ARTICLE

JunB as a potential mediator of PTHrP actions: new gene targets Ephrin B1 and VCAM-1

JE Berry[1], GJ Pettway[1,2], KG Cordell[1,3], T Jin[4], NS Datta[1,*], LK McCauley[1,3]

[1]*Department of Periodontics and Oral Medicine, School of Dentistry, University of Michigan, Ann Arbor, MI, USA;* [2]*Department of Biomedical Engineering, College of Engineering, University of Michigan, Ann Arbor, MI, USA;* [3]*Department of Pathology, Medical School, University of Michigan, Ann Arbor, MI, USA;* [4]*Department of Cariology, Restorative Sciences and Endodontics, School of Dentistry, University of Michigan, Ann Arbor, MI, USA*

Parathyroid hormone-related protein (PTHrP) is an integral mediator of physiologic and pathologic processes and has demonstrated actions in the periodontium. PTHrP functions via AP-1, and specifically through JunB. This study identified JunB-dependent downstream mediators of PTHrP using OCCM cementoblastic transfectants with JunB over- or reduced expression. Over-expressing cells showed an increase in proliferation, while the opposite was seen in siRNA transfected cells. Microarray analysis of over-expressing cells revealed more than 1000 regulated genes. Three genes were investigated in more detail. The PTH/PTHrP receptor (PTHR1) and ephrin B1 (EfnB1) were down-regulated, and vascular cell adhesion molecule-1 (VCAM-1) was up-regulated with JunB over-expression. JunB siRNA transfectants had increased PTHR1, but reduced ephrin B1 and unaltered VCAM-1 *in vitro*. To validate these targets, parental OCCM cells and primary osteoblasts were treated with PTHrP, resulting in reduced PTHR1 and ephrin B1, and increased VCAM-1. Cell transfectants were implanted subcutaneously *in vivo*, and microarray analysis and RT-PCR performed. Over-expression of JunB down-regulated PTHR1 and ephrin B1, and increased VCAM-1. JunB siRNA transfectant implants had increased PTHR1 and ephrin B1, but no altered VCAM-1. These data highlight new gene targets for PTHrP and indicate JunB is a critical mediator of PTHrP actions.
Oral Diseases (2008) **14**, 713–726

Keywords: parathyroid hormone-related protein; parathyroid hormone; cementum; bone; junB

Correspondence: Dr LK McCauley, Department of Periodontics and Oral Medicine, School of Dentistry, Room 3343, University of Michigan, 1011 North University Avenue, Ann Arbor, MI 48109 1078, USA. Tel: 734 763 2105, Fax: 734 763 5503, E-mail: mccauley@umich.edu
*Present address: Department of Internal Medicine, Wayne State University, Detroit, MI, USA.
Received 6 June 2008; revised 28 July 2008; accepted 3 August 2008

Introduction

Parathyroid hormone-related protein (PTHrP) is an autocrine, paracrine or intracrine factor during normal development and pathologic conditions (Fiaschi-Taesch and Stewart, 2003). PTHrP binds to the PTH/PTHrP receptor (PTHR1) on osteoblasts and cementoblasts to invoke numerous downstream genes in a similar manner as PTH, which binds to the same receptor (Gensure *et al*, 2005). Signaling through the PTHR1 is primarily through the PKA pathway, but the PKC and the MAPK pathways also participate in PTH and PTHrP actions in bone (Gensure *et al*, 2005).

Members of the AP-1 family of transcription factors have prominent roles in skeletal development and homeostasis (Eferl and Wagner, 2005). More than 45 genes important in bone have AP-1 sites in their promoter region (Yamashita and McCauley, 2006), and gene deletion and transgenic models of AP-1 factor over-expression have revealed critical roles for Fos and Jun family members in osteoblastic and osteoclastic cell lineages (Jochum *et al*, 2001). PTH and PTHrP treatment of osteoblasts results in a dramatic up-regulation of AP-1 family members (Yamashita and McCauley, 2006), and previous studies from our laboratory have characterized the AP-1 response in osteoblasts and cementoblasts (Berry *et al*, 2006). Cementoblasts are mesenchymal cells located on the tooth root surface which have osteoblast phenotypic characteristics (Saygin *et al*, 2000). PTHrP binds to its receptor on cementoblasts and up-regulates all of the Fos family members, but only the JunB protein of the Jun family (Berry *et al*, 2006). JunB has been found to function in osteoblasts, osteoclasts, and cementoblasts (Kenner *et al*, 2004; Berry *et al*, 2006); hence identifying the downstream genes that PTH and PTHrP activate through JunB would be a valuable aid in exploring the effect of these important compounds on mineralized tissues.

Parathyroid hormone and PTHrP support osteoclastogenesis via the up-regulation of RANKL and down-regulation of osteoprotegerin (OPG) (Lee and

Lorenzo, 1999), and PTHrP is critical for the support of osteoclasts in the developing alveolar bone, as mice with compromised PTHrP signaling lack tooth eruption (Philbrick *et al*, 1998). Unlike osteoblasts, cementoblasts do not normally support osteoclastogenesis, however PTHrP influences osteoclastogenesis by cementoblasts at least in part through PTHrP's action via JunB. Cementoblasts produce high levels of osteoprotegerin, and JunB activation via PTHrP results in a diminution of OPG and a resulting increase in osteoclastogenesis (Boabaid *et al*, 2004). However, neither the diminution of OPG nor an up-regulation of RANKL can explain the entirety of PTHrP actions. The purpose of the current study was to identify novel downstream mediators of PTHrP action via its up-regulation of JunB in a mesenchymal cementoblastic cell line *in vitro*, and validate these findings in an *in vivo* implant model.

Materials and methods

Cell culture and transfection

A subclone of the OsteoTag mouse-derived cementoblast cell line named OCCM.30 (OCCM) was cultured as previously described (D'Errico *et al*, 2000). Briefly, cells were maintained in DMEM (Invitrogen, Carlsbad, CA, USA) supplemented with 10% fetal bovine serum and 100 U ml^{-1} penicillin and 100 μg ml^{-1} streptomycin (Invitrogen) at 37°C in a humidified atmosphere of 5% CO_2. Primary calvarial cells were isolated as previously described and cultured under the same conditions (Koh *et al*, 1999).

Constructs were developed for over- and under-expression of JunB as previously described (Berry *et al*, 2006). For over-expression of JunB, full-length *junB* was cloned into pEF6/V5-His TOPO TA expression vector (Invitrogen). The JunB over-expressing vector or a vector alone control was transfected into OCCM cells using a cationic lipid reagent (Lipofectamine 2000; Invitrogen) and stable transfectants were established then subcloned. Levels of JunB over-expression in transfectants were measured using an AP-1 specific ELISA (Active Motif, Carlsbad, CA, USA), and also by Western hybridization. Subclones were screened on the basis of expression level, and subclones of each line (over-expressing and vector) were selected for further study, hereafter referred to as over-expressing Jun B (OEJB.8) and vector control (OEV) respectively. OEJB.8 exhibited an approximately 7-fold increase in JunB expression as compared with the OCCM parental clone and OEV. For reduced expression of JunB, a custom pool of *junB* siRNA constructs were made by Dharmacon Research (Lafayette, CO, USA), which was employed in transient transfection experiments using a cationic lipid reagent (Oligofectamine, Invitrogen). The most effective sequence for silencing from the pool was determined to be GGATCCCAAATGCGCTCCTGGTCTTCCATTGATATCCGTGGAAGACCAGGAGCGCATTTTTTTTTCCAAAAGCTT. This was synthesized by GenScript (Piscataway, NJ, USA) and cloned into siRNA expression vector pRNAT-U6.1/Neo for stable transfection. The negative control was a nonsense construct, pRNAU-6.1/Neo/CTL, also from Genscript, containing sequence GGATCCCGTCGCTTACCGATTCAGAATGGTTGATATCCGCCATTCTGAATCGGT. The silencing constructs and controls were transfected into OCCM cells using Lipofectamine 2000 (Invitrogen), and stable transfectants were established and subcloned. Levels of JunB under-expression were measured as above, and subclones of each line (under-expressing and nonsense control) were selected for further study, hereafter referred to as Si6.1 and control SiV. Si6.1 exhibited a level of JunB expression approximately half that of the vector control.

For PTHrP treatment experiments, cells were plated at 2×10^4 cells cm^{-2} in 60-mm dishes in DMEM supplemented as described above. On day 4 after plating, medium was switched to DMEM with 5% FBS, and on day 7 cells were treated with vehicle control or 100 nM PTHrP (1–34) (Bachem, King of Prussia, PA, USA) for various time periods, after which cells were harvested for protein or RNA isolation.

Cell enumeration and apoptosis

To determine cell numbers over time, cells were plated at a density of 1.04×10^3 cm^{-2} in 6-well plates. Beginning on day 3 after plating, triplicate wells were trypsinized and counted daily for 7 days using trypan blue exclusion to determine viability.

To evaluate apoptosis, cell transfectants were plated at approximately 2.4×10^4 cm^{-2} in 100 mM dishes and 2 days later harvested after a PBS wash, by scraping in CelLytic MT mammalian tissue lysis extraction reagent (Sigma-Aldrich, St Louis, MO, USA) with 1% Protease Inhibitor Cocktail (Sigma). Lysates were incubated on ice for 30 min with vortexing every 10 min, then centrifuged at 22 000 ***g*** at 4°C for 20 min. Supernatants were stored at −80°C until analyzed via Western blotting. Cell viability as measured by trypan blue dye exclusion was verified to be similar in parallel cultures of the transfectants. Positive controls included OEV cells treated with the pro-apoptotic agent staurosporine (25 nM) (Sigma) for 6 h.

Western blot analysis was performed after running 30 μg of each sample on 10% acrylamide gels. Filters were blocked for 1 h in 5% non-fat milk in Tris-buffered saline with Tween-20 (TBST), probed overnight with caspase 3 (Becton Dickinson, Franklin Lakes, NJ, USA) and poly(ADP-ribose) polymerase-1 (PARP-1) (Cell Signaling, Danvers, MA, USA) antibodies, then rinsed with TBST and probed with appropriate secondary antibodies (GE Healthcare, Piscataway NJ, USA). After extensive rinsing with TBST, filters were incubated with enhanced chemiluminescence reagents (Pierce Biotechnology, Rockford, IL, USA) and exposed to BioMax film. Bands were normalized with actin, and compared using either Scion Image analysis program (Scion Corporation, Frederick, MD, USA) or a Chemidoc visualization/quantification system (Bio-Rad Laboratories, Hercules, CA, USA). Relative band densities were evaluated using InStat statistical analysis program (GraphPad, San Diego, CA, USA).

In vivo *experiments*
All animals were maintained in accordance with NIH and institutional animal care guidelines, and experimental protocols were approved by the Institutional Animal Care and Use Committee of the University of Michigan. Transfected cell lines were implanted subcutaneously in a similar manner as previously described for bone marrow stromal cells (Pettway *et al*, 2005). Briefly, 1×10^6 cells were placed in a gelfoam carrier sponge and implanted over the backs of athymic nude mice (Harlan, Indianapolis, IN, USA) under anesthesia. Four weeks later, mice were sacrificed and implants were removed and either prepared for histology or immediately frozen at −70°C for further processing and evaluation of RNA.

Protein isolation and analysis
For determination of JunB levels, nuclear extracts were prepared and analyzed using both the TransAM AP-1 Family Transcription Factor Assay System (Active Motif) and Western hybridization (Novex gels; Invitrogen). Briefly, cells were collected in cold PBS in the presence of phosphatase inhibitors and resuspended in a hypotonic buffer. Detergent was added to cause leakage of cytoplasmic proteins into the supernatant, which was removed. Nuclei were lysed and nuclear proteins were solubilized in a lysis buffer containing protease inhibitors. Samples were stored at −70°C until the assays were performed. Total protein levels were equalized as measured using a Bradford-based assay (Bio-Rad), and specific ELISA and Western hybridization were performed to detect JunB. ELISAs were performed a minimum of three times, and protein expression data were analyzed using InStat statistical software (GraphPad). Western blots were performed a minimum of three times, and actin was measured in each sample as a loading control (both antibodies Santa Cruz Biotechnology, Santa Cruz, CA, USA). Western films were scanned, and relative protein expression was quantified using either Scion Image analysis program (Scion Corporation) or a Chemidoc visualization/quantification system (Bio-Rad). Relative band densities were evaluated using InStat.

RNA isolation and analysis
RNA from both cells and implants was isolated using Trizol (Invitrogen) and phase-lock gel (Eppendorf, Westbury, NY, USA). In the case of cells, Trizol was added directly to the plate, cells were scraped, and solution was transferred to a tube containing phase-lock gel for further processing. In the case of implants, the tissue, flash frozen in liquid nitrogen immediately after removal from the mouse, was crushed in liquid nitrogen, mixed with Trizol, and this mix of tissue and Trizol was then transferred to a tube containing phase-lock gel. In both cases, samples were centrifuged, precipitated in isopropanol, resuspended in DEPC-treated water, and quantified spectrophotometrically. RNA samples to be examined by microarray or real-time RT-PCR were further purified, including treatment with DNAse using an RNeasy kit (Qiagen, Valencia, CA, USA).

For Northern hybridization, 2–3 μg of RNA was denatured, fractionated by electrophoresis on 1.2% agarose 6% formaldehyde gel, transferred to a nylon membrane (Duralon, Stratagene, La Jolla, CA, USA), and cross-linked by UV radiation. Blots were hybridized with random-primed [α^{32}-P] labeled probes (Rediprime; GE Healthcare) and were exposed to Kodak X-Omat or Biomax film with intensifying screens at −70°C for 4–24 h. Probes used included bone sialoprotein (BSP) (Young *et al*, 1994), osteocalcin (OCN) (Celeste *et al*, 1986), and *junB* (McCabe *et al*, 1995). A cDNA for 18S rRNA was used to probe and normalize blots. Northern blot experiments were repeated a minimum of three times using independent RNA samples, films were scanned, and relative gene expression was quantified using Scion Image analysis program (Scion Corporation) after subtraction of background. Data were analyzed using InStat statistical software (GraphPad).

For microarray analysis, total RNA samples were evaluated spectrophotometrically to determine concentration and purity, and RNA integrity was validated by running on an agarose gel. Ten microgram of total RNA was quantitatively amplified and biotin-labeled according to the GeneChip Expression Analysis Technical Manual (Affymetrix, Inc., Santa Clara, CA, USA). Briefly, RNA was converted to double-stranded complementary DNA (cDNA) using SuperScript II RT (Invitrogen), with a T7-$(dT)_{24}$ primer (Affymetrix). The cDNA was then used in an *in vitro* transcription reaction in the presence of biotin-modified ribonucleotides (Enzo, Farmingdale, NY, USA) to produce large amounts of single stranded RNA. Biotin-labeled RNA was fragmented and 10 μg was hybridized to GeneChip array 'Mouse Genome 430A' (Affymetrix) at 45°C for 16-h. Labeled bacterial RNAs of known concentration were spiked in hybridization to generate an internal standard and to allow normalization between chips. Chips were washed and stained with streptavidin R-phycoerythrin (Molecular Probes, Eugene, OR, USA). After scanning the chips, the data were analyzed by using Affymetrix GeneChip related software including GCOS and Data Mining Tool. The microarray experiments were performed three times (*in vitro* samples twice, *in vivo* samples once) and selected genes were validated by real-time RT-PCR.

Real-time quantitative RT-PCR utilized the ABI 7500 system (Applied Biosystems, Foster City, CA, USA). For reverse transcription (RT), a 25 μl RT reaction with 0.5 μg total RNA and random hexamers was performed using TaqMan® Reverse Transcription Reagents (Applied Biosystems). PCR was performed by using TaqMan® Universal PCR Master Mix (Applied Biosystems). Briefly, a 30 μl PCR reaction was prepared with 1 μl cDNA (RT product) and 1.5 μl mixture of TaqMan Gene Expression Assays probe and primers mixture, specified as follows: PTHR1 ABI# Mm00441046_m1 with probe sequence CTGCACACAGCAGCCAACATAATGG, NBI Accession# NM_011199.1; VCAM1 ABI# Mm00449197_m1 with probe sequence GGAGGTCTACTCATTCCCTGAAGAT, NBI Accession no. NM_011693.2; EfnB1 ABI#

Mm00438666_m1 with probe sequence CTGGAGCT-CTCTTAACCCTAAGTTC, NBI Accession # NM_010110.2. Thermal conditions were: 50°C 2 min, 95°C 10 min followed by 40 cycles of 95°C 15 s and 60°C 1 min. Expression levels of genes of interest were normalized by comparison to TaqMan Rodent GAPDH Control Assay of each sample. Real-time RT-PCR was repeated a minimum of three times with similar results.

Results

Over-expression of JunB increases, and silencing inhibits, proliferation in cementoblasts

The OCCM cementoblastic cells were easily transfected, and numerous subclones of JunB over-expressing and siRNA lines were generated. Cell lines were screened at the RNA and protein levels to validate the expected altered gene expression (Figure 1). Several cell lines were evaluated in the various assays, and selected clones are shown. The OEJB.8 subclone of JunB over-expressing cells displayed an approximately 7-fold increase in mRNA for *junB* and an approximately 2-fold increase in protein levels compared with OEV, the vector control. The Si6.1 subclone of JunB siRNA cells displayed a 45% decrease in mRNA for *junB* and a 50% decrease in protein levels compared with its vector control, SiV. As AP-1 family members have been reported to alter cell proliferation, an evaluation of cell numbers over time was performed. Over-expression of JunB resulted in increased cell numbers after 5 days (Figure 2a). In contrast, knock down of JunB resulted in lower numbers of cells over time (Figure 2b). Western hybridization analysis examining cleavage of PARP-1 and caspase-3 were performed to characterize the difference in cell numbers relative to apoptosis (Figure 2c). The OEJB.8 transfectants showed a small but detectable band of cleaved PARP, however there was no significant cleavage of PARP-1 or caspase-3 in any of the cell transfectants either over- or under-expressing JunB, suggesting that apoptosis was not a prominent occurrence under the culture conditions. These data indicate that the increase in cell numbers associated with JunB over-expression is not because of reduced apoptosis, but instead because of changes in proliferation.

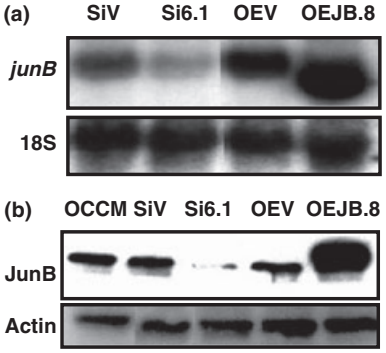

Figure 1 JunB levels in transfectants. (**a**) Northern blot analysis of *junB* mRNA levels from OCCM cell transfectants, (**b**) Western blot analysis of JunB protein levels in nuclear extracts from OCCM cell transfectants. The vector control cells for both the JunB silencing (SiV) and over-expression (OEV) showed similar protein levels of JunB as the parental OCCM cells. JunB silenced cells (Si6.1) had reduced JunB mRNA and protein, while over-expressing cells (OEJB.8) had higher JunB as compared with the respective vector controls

Genes altered by JunB up-regulation in vitro*, PTHR1, VCAM-1 and EfnB1, identified by microarray and validated by real-time RT-PCR*

AP-1 sites are present in a wide variety of genes, many of which are important in mineralized tissues (Yamashita and McCauley, 2006). To elucidate genes that are specific targets of JunB action, a microarray analysis was performed on the OCCM transfectants that over-expressed JunB as compared with control transfectants. There were more than 600 genes identified as being up-regulated 2-fold or more by JunB and more than 750 genes identified as being down-regulated 2-fold or more by JunB (Table 1 and Supporting information). If genes were detected more than once per chip, the fold change is seen as an average of the values.

Several genes of interest were studied further, and three were evaluated in detail and presented here. The PTHR1 was selected because it was found to be highly down-regulated by JunB over-expression in the microarray (28-fold) and because it is well known to be down-regulated by PTH and PTHrP at the RNA level, but very little information exists regarding the operative transcriptional mediators. JunB over-expression nearly abolished expression of the PTHR1 as measured by real-time PCR and a 2.5-fold increase in the PTHR1 was found in the *junB* siRNA transfectants as compared with the control transfectants (Figure 3a). Vascular cell adhesion molecule-1 (VCAM-1) was selected because it was found to be up-regulated 3-fold in the microarray data with over-expression of JunB, because it has not yet been reported to be mediated by PTHrP, and because of its reported role in osteoclastogenesis (Michigami *et al*, 2000). Validation by RT-PCR revealed an approximately 2.5-fold up-regulation of VCAM-1 by JunB over-expression, however no regulation was found when JunB was silenced (Figure 3b). Ephrin B1 (EfnB1) was selected because it was down-regulated 5-fold by the over-expression of JunB in OCCM cells in the microarray analysis, because it had not been previously reported to be a PTHrP target and because of its novel role in craniofacial development (Twigg *et al*, 2004). Ephrin B1 was dramatically down-regulated by JunB over-expression as confirmed by RT-PCR with levels at 10% of controls (Figure 3c). However, silencing JunB did not result in an opposite effect, as siRNA for JunB also resulted in down-regulation of Ephrin B1 *in vitro* as measured by RT-PCR, although to a much lesser extent.

Silencing of JunB attenuates PTHrP effects in cementoblasts

To determine if the reduction in JunB compromised the PTHrP effects on these genes, OCCM parental cells and JunB silenced (Si6.1) or vector control (SiV) cells were treated with PTHrP or vehicle and RNA isolated and analyzed by real-time PCR. The PTHR1 and

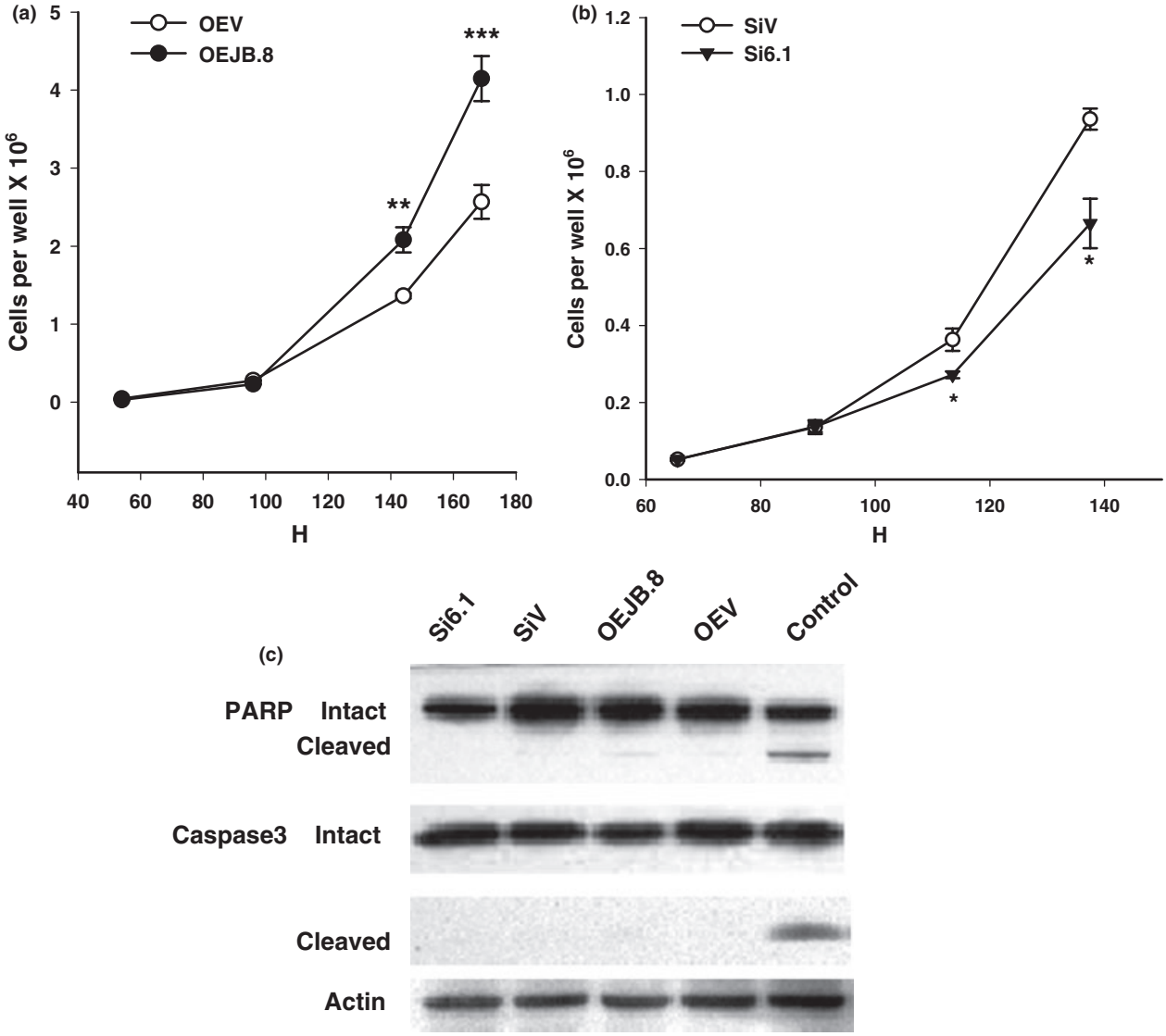

Figure 2 Proliferation of JunB transfectants. OCCM transfectants were plated at 1×10^3 cells cm^{-2} and cell numbers determined over time. (**a**) JunB over-expressing transfectants, (**b**) JunB siRNA transfectants. Over-expression of JunB caused an increase in cell numbers, while silenced cells exhibited lower cell numbers over time as compared with vector controls. Data is expressed as mean ± s.e.m. of triplicate samples. $^{***}P < 0.001$ *vs* OEV control, $^{**}P < 0.01$ *vs* OEV control, and $^{*}P < 0.05$ *vs* SiV control, (**c**) Western blot for apoptotic markers in JunB transfectants. Each lane loaded with 30 μg protein; positive control was OEV cells treated for 6 h with 25 nM staurosporine. There were no differences in cleaved PARP-1 or caspase-3 in transfectants

ephrin B1 responses were attenuated (Figure 3d). When JunB was silenced, PTHrP treatment did not lower the PTHR1 or ephrin B1 levels to the same extent as it did in controls, suggesting that JunB is key for the gene effects. Interestingly, the VCAM levels were similar and elevated with PTHrP regardless of JunB silencing, suggesting JunB may not be the only factor to contribute to the PTHrP mediated increase in VCAM-1 (Figure 3e).

Increase in junB expression levels precede effects of PTHrP on PTHR1, EfnB1 and VCAM-1 in cementoblasts and osteoblasts

To substantiate that JunB regulation resulted in downstream gene alterations that were consistent with a PTHrP effect, parental OCCM cells were treated with PTHrP and gene expression for PTHR1, VCAM-1 and Ephrin B1 was measured by RT-PCR over time. There was significant down-regulation of PTHR1 and ephrin B1 at 4 and 8 h (Figure 4a). PTHR1 remained significantly down-regulated at 24 h, while ephrin B1 recovered slightly (not shown). VCAM-1 mRNA levels were significantly up-regulated by PTHrP at 4 and 8 h (Figure 4a), and stayed significantly elevated at 24 h. To compare the PTHrP impact on cementoblasts with osteoblasts, similar experiments that focused on the early time-points where the greatest change was found were performed with primary osteoblastic cells *in vitro*. Osteoblasts displayed a similar trend with increased expression of

Table 1 Microarray data of cell transfectants *in vitro* microarrays were performed using RNA isolated from JunB over-expressing cells (OEJB.8) or vector control (OEV)

GenBank no.	*Gene name*	*Fold change*
AV152334	ATPase, Na^+K^+ transporting, beta 1 polypeptide	+16
AW494038	Calcium channel, voltage-dependent, T type alpha 1G subunit	+10
NM_018857.1	Mesothelin	+7
BB357126	Serinethreonine kinase 11	+7
NM_011361.1	Serumglucocorticoid regulated kinase	+6
BC002081.1	Jun oncogene	+4
NM_010107	Ephrin A1	+4
NM_011693.1	**Vascular cell adhesion molecule 1**	+3
NM_008597.1	Matrix gla protein	+3
XM_892839	Ephrin A3	+3
NM_007910	Ephrin A4	+2
BI110565	Osteoblast specific factor 2	−246
NM_021355.1	Fibromodulin	−50
BC013446.1	**PTH receptor-1**	−28
NM_008480.1	Laminin, alpha 1	−27
AW319615	Alkaline phosphatase 2	−20
NM_008318.1	Bone sialoprotein	−16
BC019502.1	Biglycan	−10
BB280300	Myocyte enhancer factor 2C	−10
BC019836.1	Insulin-like growth factor binding protein 4	−9
NM_011607.1	Tenascin	−9
NM_009982.1	Cathepsin C	−8
NM_010207.1	Fibroblast growth factor receptor 2	−7
NM_008393.1	Iroquois related homeobox 3	−7
BI111620	Tissue inhibitor of metalloproteinase 3	−7
NM_012050.1	Osteomodulin	−6
NM_010110.1	**Ephrin B1**	−5
NM_007541.1	Osteocalcin	−5
BB732264	Cadherin 2	−4
NM_130458.1	Osterix	−4
U65020.1	Dentin matrix protein 1	−2

A selected list of genes altered by JunB over-expression is provided here (see Supporting information for more extensive list). Genes evaluated in detail are indicated in bold. For genes detected more than once in the array, fold change is expressed as an average of all readings.

VCAM-1 and reduced expression of ephrin B1 and PTHR1 (Figure 4c). Notably, in all studies osteoblasts had higher baseline values of VCAM-1 than cementoblasts, and although they did display a PTHrP-mediated increase in VCAM-1, they did not have as dramatic an up-regulation in response to PTHrP. Gene expression for *junB* in response to PTHrP followed an earlier time course consistent with *junB* preceding the downstream gene expression. Maximal expression of *junB* in response to PTHrP in cementoblasts and osteoblasts was 1–2 h (Figure 4b,d).

Effects of JunB over-expression evaluated in vivo

In vitro model systems are powerful tools to identify gene targets and begin to sort out mechanisms of protein action, but at times do not always replicate the *in vivo* state because of a plethora of other cells and factors that can modify target gene expression. To validate the *in vitro* findings in the context of a whole animal, OCCM transfectants were implanted subcutaneously into immunocompromised mice. Cementoblast implants were examined histologically and mRNA was isolated and gene expression analyzed by microarray and real-time PCR. Control implants presented with a well-defined proliferation of cells with round to elongated basophilic nuclei (Figure 5a,c,e). A prominent accumulation of eosinophilic calcified material consistent with osteoid or cementum was found forming a fine meshwork of trabeculae lined by cells with hyperchromatic angular nuclei. Cells were also contained within lacunar spaces within the calcified material similar to osteocytes or cementocytes. Numerous small vascular channels were observed throughout the control specimens. Implants with cells over-expressing JunB (Figure 5b,d) presented as densely cellular with a brisk mitotic rate, abundant pleomorphism, less vascularity than vector implants and lacked visible mineralization. A pale-staining, basophilic acellular material representing residual gelfoam scaffold was found in the JunB over-expressing implants but very little in other implants. The implants with silencing transfectants appeared similar to the vector controls. (Figure 5f).

The overall size of the implants upon gross examination revealed reductions in the size of implants that contained either the JunB over-expressing or the silenced transfectants (Figure 5g). To ascertain the impact of JunB on parameters of differentiation relative to cell mineralization, OCN gene expression was determined in implants from transfectants. Silencing of JunB led to increased OCN whereas over-expression of JunB led to a dramatic down-regulation of OCN (Figure 5h).

Microarray analysis of gene expression influenced by JunB in vivo *examined and validated by real-time RT-PCR*

Microarray analysis of implants from mice with over-expressing transfectants revealed more than 700 genes up-regulated 2-fold or greater and more than 1250 genes down-regulated (Table 2 and Supporting information). If genes were detected more than once per chip, the fold change is seen as an average of the values. Similar to the *in vitro* findings, the PTHR1 was nearly abolished by JunB over-expression, whereas silencing resulted in an up-regulation of the PTHR1 as determined by real-time PCR (Figure 6a). Over-expression of JunB in implants resulted in a dramatic 8-fold increase in VCAM-1 but no alteration was found with silencing of JunB *in vivo* (Figure 6b). Ephrin B1 was down-regulated 3-fold *in vivo* with JunB over-expression and, unlike the results found *in vitro*, up-regulated significantly with JunB silencing (Figure 6c).

Comparison of genes regulated in vivo *and* in vitro

A comparison of genes regulated *in vitro* and *in vivo* was performed as a means to better understand the JunB gene targets (Table 3 and Supporting information). Of note, genes associated with late stages of mineralization such as BSP, OCN and dentin matrix protein-1 (DMP-1) were down-regulated, and to a greater extent *in vivo*

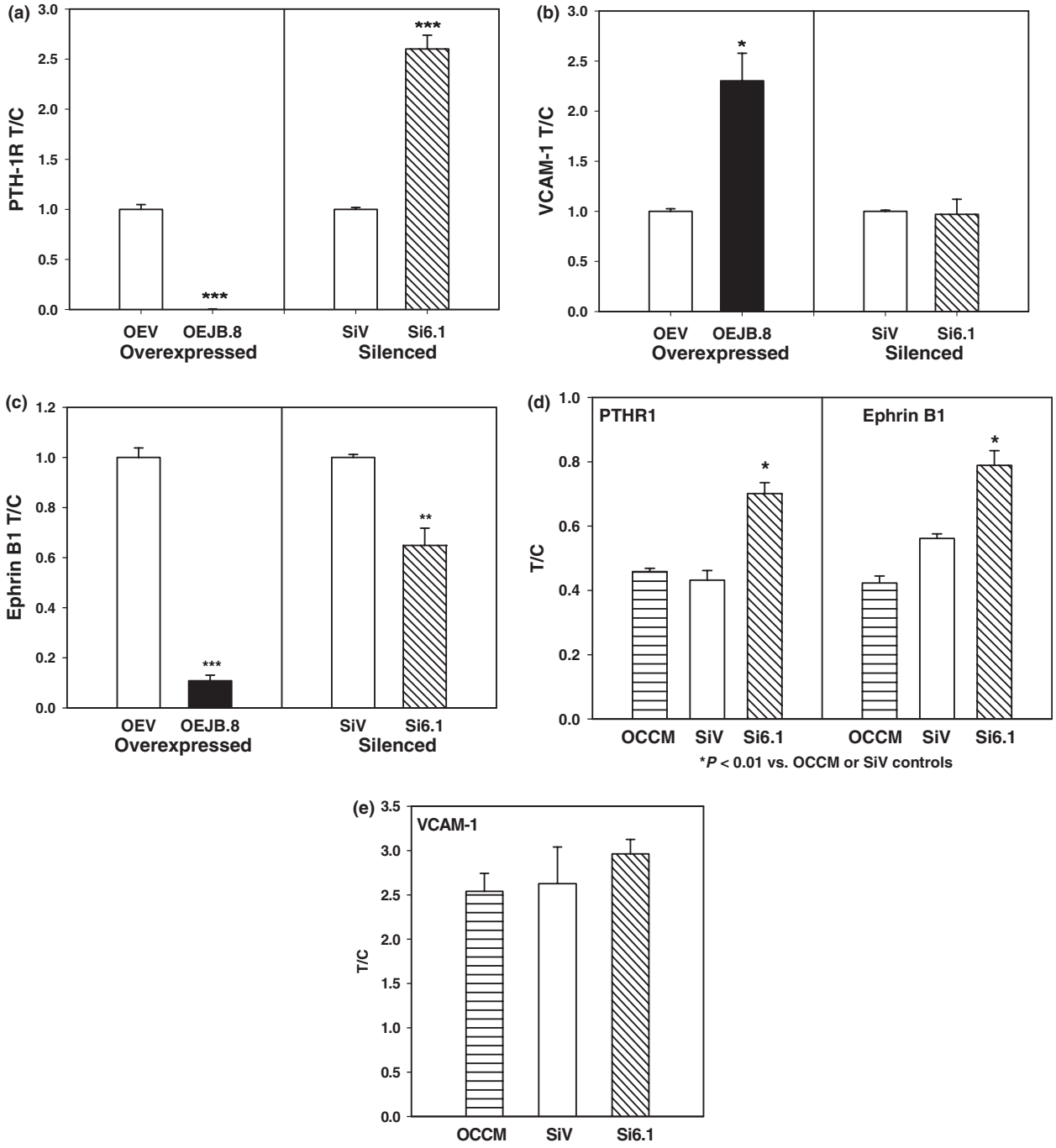

Figure 3 Real-time PCR validation of three selected genes identified in microarray analysis from transfectants *in vitro*. (**a**) PTHR1 gene expression in JunB over-expressing (OEJB.8) and vector control (OEV) cells (left), PTHR1 gene expression in JunB siRNA (Si6.1) and vector control (SiV) cells (right), (**b**) VCAM-1 gene expression in OEJB.8 and OEV cells (left), VCAM-1 gene expression in Si6.1 and SiV cells (right), (**c**) Ephrin B1 gene expression in OEJB.8 and OEV cells (left) Ephrin B1 gene expression in Si6.1 and SiV cells (right). (**d**) PTHR1 (left) and Ephrin B1 (right) or, (**e**) VCAM-1 gene expression in response to PTHrP treatment (100 nm; 4 h) in parental OCCM, SiV or Si6.1 cells. (**a–c**) Data is expressed as mean ± s.e.m. of triplicate samples and assays repeated at least four times with similar results. (**d**, **e**) Data is expressed as treatment over control (T/C) of triplicate samples and mean ± s.e.m. with assays repeated at least two times with similar results. ***$P < 0.001$ *vs* respective vector control, **$P < 0.01$ *vs* respective vector control, *$P < 0.05$ *vs* respective vector control

than *in vitro*. Furthermore, the inhibitor of mineralization, matrix gla-protein was up-regulated. This suggests that JunB is associated negatively with mineralization, but could also reflect a later stage of cell differentiation operative in the *in vivo* model.

Discussion

The present study identified new gene targets of PTHrP that are downstream of JunB in cementoblast cells and characterized these both *in vitro* and *in vivo*. PTH and

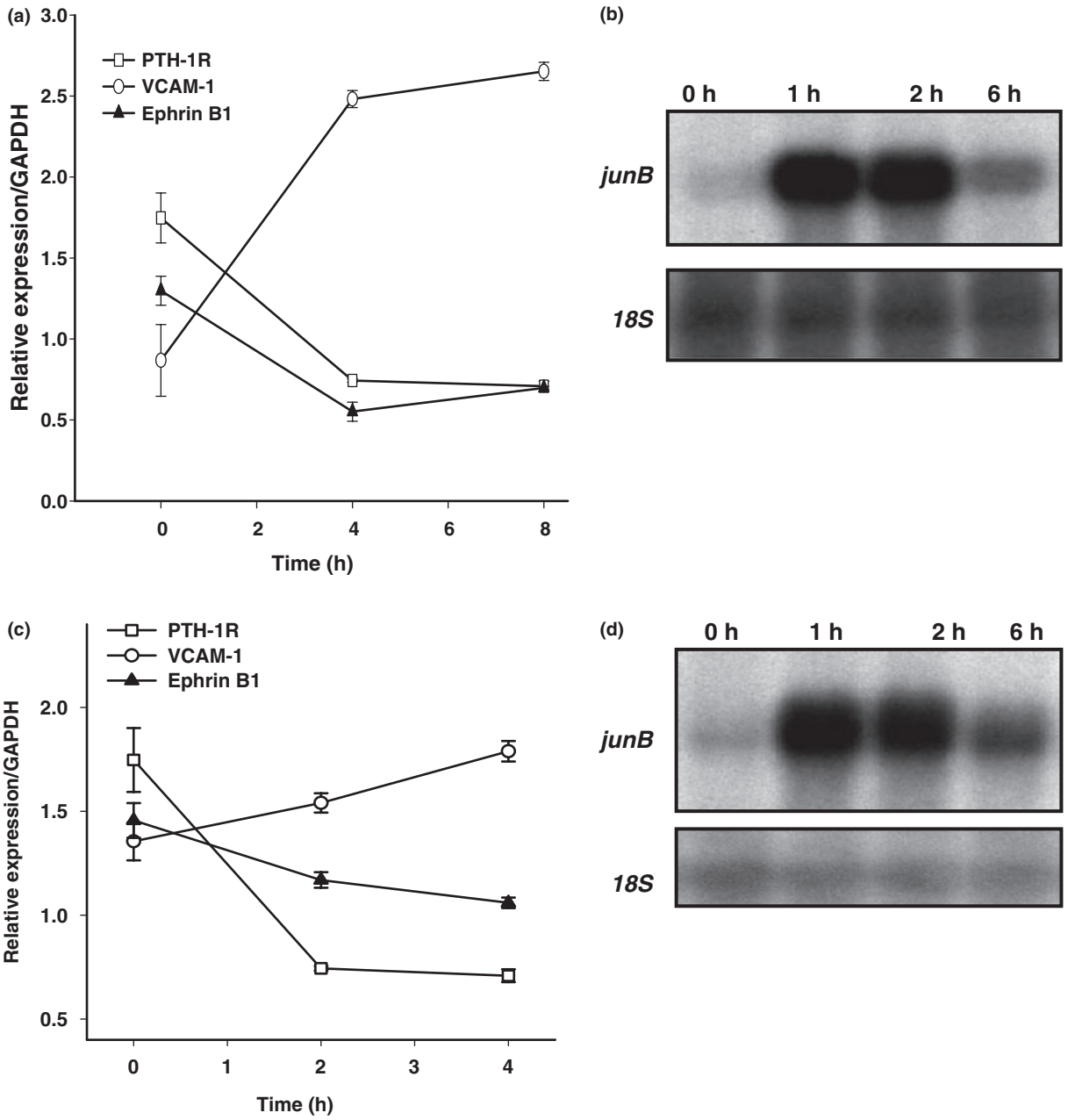

Figure 4 Time course of PTHrP action on OCCM cell gene expression *in vitro* for PTHR1, VCAM-1, and Ephrin B1. (**a**) Parental OCCM cells were treated for 0–8 h with 100 nM PTHrP and gene expression measured by realtime RT-PCR. PTHR1 levels were 2.4-fold lower at 4 hand 2.5-fold lower at 8 h ($P < 0.001$ *vs* time zero). Ephrin B1 levels were 2.4-fold lower at 4 h and 1.9-fold lower at 8 h ($P < 0.05$ *vs* time zero). VCAM-1 levels were 2.9-fold higher at 4 h and 3.1-fold higher at 8 h ($P < 0.05$ *vs* time zero). (**b**) Parental OCCM cells were treated for 0–6 h with 100 nM PTHrP and gene expression measured by northern blot analysis. *junB* levels were maximal at 1–2 h and decreased thereafter. (**c**) Primary murine calvarial cells were isolated and cultured to confluence, followed by differentiation with 50 μM ascorbic acid for 7 days. Cells were then treated for 0–4 h with PTHrP (100 nM) and gene expression measured by real-time RT-PCR. PTHR1 levels were 1.4-fold lower at 2 h and 2.8-fold lower at 4 h ($P < 0.001$ for both) compared with time zero. Ephrin B1 levels were 1.3-fold lower at 2 h ($P < 0.05$) and 1.4-fold lower at 4 h ($P < 0.01$) compared with control. VCAM-1 levels were 1.3-fold higher at 4 h ($P < 0.01$) compared with time zero. (**d**) Primary calvarial cells were treated for 0–6 h with 100 nM PTHrP and gene expression measured by northern blot analysis. *junB* levels were maximal at 1–2 h and decreased thereafter. Data for **a, c** are plots from representative experiments repeated 2–3 times with similar results and expressed as mean ± s.e.m. of triplicate samples. Data for **b**, **d**, are representative blots from experiments repeated a minimum of three times with similar results

PTHrP are well known for their critical biological activities during normal development and pathologic conditions in bone, specifically on target osteoblastic cells, and have also been found to be important in tooth development and eruption. PTH and PTHrP often display differing actions on downstream genes when comparing effects in various model systems. For example, PTH has been shown to have opposing effects on transformed osteoblasts *vs* primary osteoblasts, where PTH up-regulates BSP in osteosarcoma cells but down-

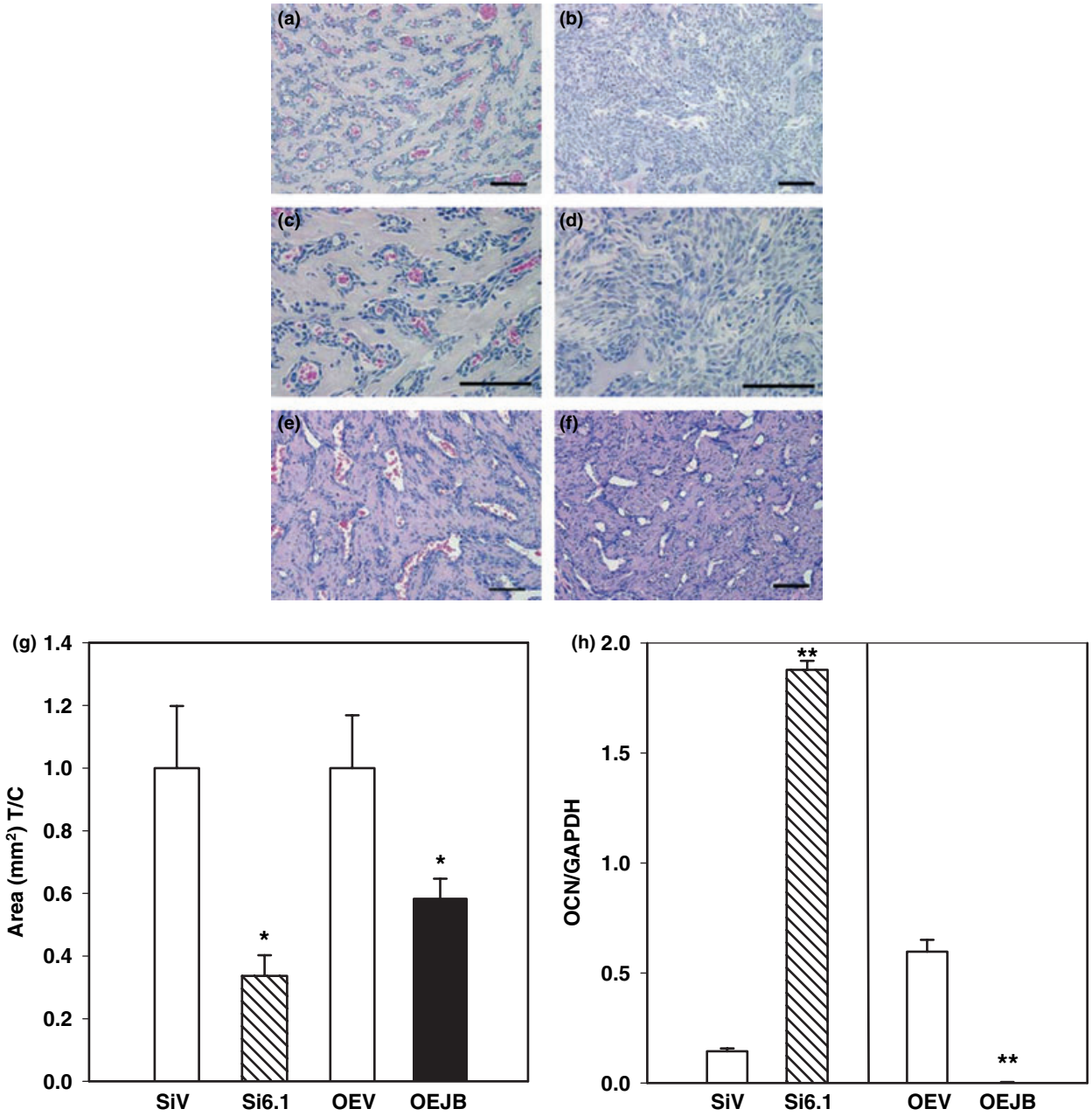

Figure 5 JunB transfectants *in vivo*. Transfectants were implanted at 1×10^6 cells/implant in collagen sponges subcutaneously and monitored for 4 weeks prior to sacrifice and histologic processing. (**a**) OEV vector control implant, (**b**) OEJB.8 JunB over-expressing cell implant, (**c**) high power view of OEV, (**d**) high power view of OEJB.8, (**e**) SiV, JunB silenced vector control, (**f**) Si6.1 JunB silenced cells. Photomicrographs of transfectants revealed increased cellularity and polyploidy in JunB over-expressing cell (OEJB.8) implants, with less vascularity and no visible mineralization as compared with vector control (OEV). Implants from JunB silenced cells (Si6.1) were similar in appearance to respective vector controls (SiV). Scale *A–F* = 100 μm. (**g**) Implant size (n = 4–7/gp) Both over-expression and siRNA for JunB resulted in smaller implants than respective controls. (**h**) Osteocalcin (OCN) expression in implants (n = 2–4/group). OCN was significantly increased in implants with siRNA knock down of JunB and significantly decreased in implants with JunB over-expressing transfectants ($P < 0.0001$ for each compared with control)

regulates it in primary calvarial cells (Yang and Gerstenfeld, 1996; Ogata *et al*, 2000). Such apparently contradictory findings have complicated the elucidation of mechanisms of action of PTH and PTHrP in mineralized tissues, but also suggest that the *in vivo* effects of PTH and PTHrP may be indirect, and hence other cellular targets may be operating in the downstream events.

Regarding a difference in pro- *vs* anti- proliferative effects of PTHrP: in differentiated osteoblastic cells the effect of PTH or PTHrP is to inhibit proliferation; however, in sparsely seeded cultures *in vitro* or in an *in vivo* implant model, PTH and PTHrP clearly lead to pro-proliferative effects (Datta *et al*, 2005, 2007; Pettway *et al*, 2008). In the present study, as the over-expressing transfectants have elevated JunB from the initiation of

Table 2 Microarray analysis of cell transfectants *in vivo*

GenBank no.	*Gene name*	*Fold change*
AV152334	Cellular retinoic acid-binding protein 2	+103
NM_053110.1	Glycoprotein (transmembrane) nmb	+29
M21836.1	Extra-embryonic endodermal cytokeratin type II	+27
NM_020265.1	Dickkopf 2	+12
M12233.1	Actin, alpha 1, skeletal muscle	+9
NM_011693.1	**Vascular cell adhesion molecule 1**	+8
NM_025711.1	Asporin	+7
AI747133	Calpain 6	+7
BI692925	Chondroitin sulfate proteoglycan 2	+6
AV152334	ATPase, Na^+K^+ transporting, beta 1 polypeptide	+3
NM_008597.1	Matrix gla protein	+3
XM_892839	Ephrin A3	+2
NM_007910	Ephrin A4	+2
BB795191	Melanoma antigen	−139
NM_008318.1	Bone sialoprotein	−67
U65020.1	Dentin matrix protein-1	−35
NM_007541.1	Osteocalcin	−21
BC022107.1	Cadherin 2	−9
AV291165	Myocyte enhancer factor 2c	−9
NM_010056.1	Distal-less homeobox 5	−7
NM_008393.1	Iroquois related homeobox 3	−7
NM_130458.1	Osterix	−7
BC013446.1	**PTH receptor-1**	−7
AW319615	Alkaline phosphatase 2	−6
NM_008592.1	Forkhead box C1	−5
NM_011607.1	Tenascin	−5
NM_010110.1	**Ephrin B1**	−3

Microarrays were performed using RNA isolated from cementicle implants in athymic mice. Implants were generated using JunB over-expressing cells (OEJB.8) or vector control (OEV). A select list of genes altered by JunB over-expression is provided here (see Supporting information for more extensive list). Genes evaluated in detail are indicated in bold. For genes detected more than once in the array, fold change is expressed as an average of all readings.

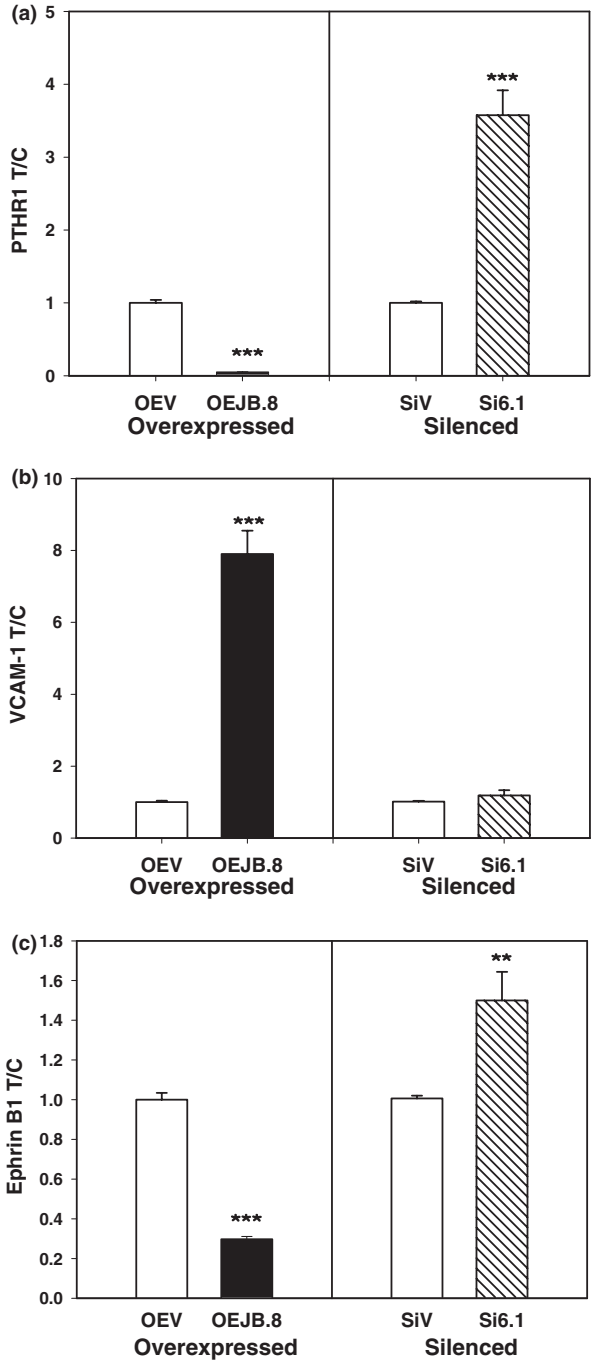

Figure 6 Real-time PCR validation of three genes identified in microarray analysis from transfectants *in vivo*. Implants of OCCM transfectants with JunB over-expressing (OEJB.8) and silenced (Si6.1) cells and their appropriate controls (OEV and SiV) were harvested after 4 weeks in nude mice. RNA was isolated, and real-time RT-PCR was performed to analyze expression of the (**a**) PTHR1, (**b**) VCAM-1 and (**c**) Ephrin B1. Results are expressed as treatment/control (T/C), and assays were performed on at least four implants each. Comparison is shown on each graph between over-expressing and silenced implants. (**a**) PTHR1 $***P < 0.001$ compared with respective controls. (**b**) VCAM-1 $***P < 0.001$ compared with respective control. (**c**) Ephrin B1 $***P < 0.001$ and $**P < 0.01$ compared with respective controls

culture, they likely display the pro-proliferative JunB effects that could be attributed to early PTHrP administration. JunB under-expressing cells, on the other hand, show a lower rate of proliferation, which is consistent with the lower proliferation rate seen in osteoblasts obtained from mice lacking JunB (Kenner *et al*, 2004). In neither case was apoptosis, as measured by PARP-1 and caspase-3 cleavage, an evident factor in influencing cell number. However, an exhaustive analysis of the proliferative and apoptotic aspects of PTHrP on mesenchymal cells was not performed in this study, as it was the focus of previous reports, as mentioned above, and as the goal for this study was to concentrate on downstream gene events.

One of the goals of the current study was to reveal new gene targets that are operative both *in vitro* and *in vivo* as a means to better identify the cellular targets and mechanisms of PTH and PTHrP actions in mineralized tissues. Three gene targets were identified and characterized in further detail. The PTHR1 has previously been identified as a down-regulated gene target of PTH and PTHrP action in bone and cementum and served in part to validate the model system. Ephrin B1 was also down-regulated and was intriguing for its known role in

Table 3 Genes regulated both *in vitro* and *in vivo*

Gene name	*Change* in vitro	*Change* in vivo
ATPase, Na^+/K^+ transporting, beta 1 polypeptide	+18	+3
Jun oncogene	+7	+2
Serum/glucocorticoid regulated kinase	+6	+3
Tubulin, beta 2b	+5	+2
Vascular cell adhesion molecule 1	+5	+8
Matrix gla protein	+3	+3
Ephrin A3	+3	+2
Ephrin A4	+2	+2
Bone sialoprotein	−16	−67
PTH receptor	−28	−7
Alkaline phosphatase 2	−20	−6
Myocyte enhancer factor 2C	−11	−10
Tenascin	−9	−5
Iroquois related homeobox 3	−7	−7
Fibroblast growth factor receptor 2	−6	−4
Ephrin B1	−6	−3
Osteocalcin	−5	−21
Cyclin-dependent kinase inhibitor 1A	−4	−3
Cadherin 2	−4	−9
Dentin matrix protein 1	−2	−35

Comparison was performed between the microarrays from JunB over-expressing cementoblast transfectants *in vitro* and their implants *in vivo*. A selected list of genes altered by JunB over-expression in both instances appears here (see Supporting information for complete list). Genes investigated in detail are indicated in bold. For genes detected more than once in the array, fold change is expressed as an average of all readings.

craniofacial development. VCAM-1 was found to be up-regulated, and this study is the first to identify it as a gene target in response to PTH or PTHrP.

The PTHR1 is a seven transmembrane domain receptor that is well characterized as being present in the PTH target organs of bone and kidney. The PTHR1 is the product of a complex gene extending over 22 kb and consisting of 15 exons and is well conserved across species (Kong *et al*, 1994). Very little has been reported of its transcriptional controls and promoter elements. PTH and PTHrP have been reported to down-regulate the PTHR1 at the mRNA level but AP-1 regulation of the PTHR1 promoter has not been described. The significance of PTH and PTHrP down-regulating their own receptor is obvious, as it forms an easily regulatable feedback system to prevent over-stimulation of the PTHR1. Constitutive activation of the PTHR1 results in the condition of Jansen's chondrodysplasia (Schipani *et al*, 1995). A notable mouse model of constitutive activation of the PTHR1 demonstrates an anabolic phenotype in trabecular bone (Calvi *et al*, 2001). That PTHrP and JunB down-regulate the PTHR1 suggest that they may be working to prevent and/or balance the PTHR1 mediation of high bone mass and/or restrict or limit the progress of tooth eruption that is dependent on PTHrP expression.

Ephrin B1 is a member of a family of ligands for ephrin receptors (Eph) (Davy and Soriano, 2005). The Eph family is the largest family of protein tyrosine kinase receptors and consists of six ephrin B receptors (EphB) and 10 ephrin A receptors (EphA) (Zhao *et al*, 2006). The cell surface ephrin Bs (ephrins B1–B3) are ligands for the EphBs and the ephrin As (ephrin A1–A5) are ligands for the EphAs. Recently there is an evidence that ephrins play critical roles in bone, and specifically in the signaling between osteoblasts and osteoclasts (Zhao *et al*, 2006). Interestingly, mutations in ephrin B1 in humans have been found to be responsible for a craniofacial abnormality called craniofrontalnasal syndrome (Twigg *et al*, 2004). Humans with this gene mutation typically have hypertelorism, a nasal groove, craniosynostosis and often present with cleft lip and palate (Wieacker and Wieland, 2005). Mice with targeted deletion of ephrin B1 are perinatal lethal (Davy *et al*, 2004). Such findings have validated a role for ephrin B1 in neural crest cell migration and in epithelial mesenchymal boundaries. Ephrins are implicated in maintaining cranial sutures, as a lack thereof has been found to result in craniosynostosis (Merrill *et al*, 2006). Expression of ephrin B1 in cementum could provide signals necessary to maintain a periodontal ligament space and prevent ankylosis. Data in the present study indicate that PTHrP, via its up-regulation of JunB, results in a reduction in ephrin B1 gene expression. Interestingly, ephrin B1 has been shown to interact with PSD-95/Dlg/ZO-1 (PDZ) binding intracellular proteins and modify G-protein-coupled receptor signaling (Lu *et al*, 2001). PDZ binding proteins have been found to be important in regulating signaling of the PTHR1 (Mahon *et al*, 2002; Sneddon *et al*, 2003). It is possible that the PTH down-regulation of ephrin B1 could be a means to auto regulate signaling of the PTHR1.

Vascular cell adhesion molecule-1 is an adhesion molecule that has been widely studied for its role in vascular formation. VCAM-1 interacts with its receptor $\alpha4\beta1$ (VLA-4) (Lobb and Hemler, 1994). VCAM-1 was first characterized for its expression on endothelial cells and its ability to promote localization of circulating lymphocytes to sites of vascular remodeling (Jin *et al*, 2006). Most immune cells including T- and B-lymphocytes and monocytes will bind to VCAM-1, and its receptor VLA-4 is important for hematopoietic stem cell renewal (Priestley *et al*, 2006). VCAM-1 has also been implicated in its ability to support osteoclastogenesis by stromal cells and in myeloma cell cultures (Feuerbach and Feyen, 1997; Michigami *et al*, 2000). Inflammatory cytokines such as interleukin-1 and tumor necrosis factors have been shown to up-regulate VCAM-1, and levels typically stay high for 48 h (Kindle *et al*, 2006). In the present study, it was found that PTHrP via its up-regulation of JunB resulted in an increase in VCAM-1 gene expression. These data suggest that PTHrP via JunB may support bone resorption and/or hematopoietic cell homing at least in part via the up-regulation of VCAM-1, and this interaction could be a key in facilitating resorption to allow for tooth eruption as well as a factor in pathologic resorption in the case of disease.

The siRNA inhibition of JunB effectively reduced the PTHrP impact on ephrin B1 and the PTHR1, as neither

were down-regulated as much as vector controls. However, the PTHrP mediated impact on VCAM-1 was unchanged in the JunB siRNA transfectants, with up-regulation by PTHrP remaining strong. It is possible that in the instance of VCAM-1 having two AP-1 sites in its promoter (Niesh *et al*, 1992) that another AP-1 family member may be compensating for the reduction in JunB. In fact, we previously reported that silencing of JunB resulted in increased levels of phosphorylated c-Jun (Berry *et al*, 2006). C-Jun often can have similar functions as JunB in target promoters, and in fact has been found to up-regulate VCAM-1 in other cell systems (Ahmad *et al*, 1998). Hence, it is possible that the decrease of JunB resulted in an up-regulation of c-Jun activity that, in the case of VCAM-1, compensated for the lack of JunB. This does not diminish that JunB could mediate PTHrP effects at the VCAM-1 promoter, but suggests that it is not the sole mediator of PTHrP effects on this gene. Future studies that dysregulate both JunB and c-Jun would be necessary to validate this. The VCAM-1 promoter has 2 AP-1 sites, and the PTHR1 and the ephrinB1 promoter both have truncated AP-1 sites (Korenaga *et al*, 1997; Manen *et al*, 1998; Brown, 2007). Such truncated sites have been found to be functional, but as with all AP-1 sites the effects are cell context dependent (Chinenov and Kerppola, 2001; Zhou *et al*, 2005).

The design of this study enabled interesting comparisons between *in vitro* and *in vivo* model systems and between the over-expression and knock down of JunB. The three genes selected are regulated both by JunB and PTH/PTHrP, and include a known gene regulated by PTH and PTHrP and two novel genes, one of which was up-regulated and one down-regulated by JunB. The pattern of responses was different for all three genes. Regulation of the PTHR1 by JunB was strong and consistent both *in vitro* and *in vivo*: over-expression of JunB down-regulated the receptor *in vitro* and *in vivo* and silencing JunB increased the receptor expression in both cases. PTH and PTHrP down-regulation of their receptor at the mRNA level has been reported (Koh *et al*, 1999; Gensure *et al*, 2005), but the JunB mediation of this had not previously been investigated. Although c-Jun can replace the action of JunB in many circumstances, the data in the present study suggest that JunB is essential for expression of the PTHR1. VCAM-1 expression was up-regulated by the over-expression of JunB both *in vitro* and *in vivo* but silencing of JunB had no effect on VCAM-1 in either situation. This suggests that JunB is permissive for VCAM-1 expression but not essential, and that other Jun family members may substitute for the lack of JunB and/or that even low levels of JunB are sufficient to drive baseline values of VCAM-1. Ephrin B1 levels were down-regulated with over-expression of JunB both *in vitro* and *in vivo*, but silencing of JunB resulted in disparate results. *In vivo* JunB silencing resulted in an expected opposite response to over-expression with increased ephrin B1 expression. However, *in vitro*, cells with JunB siRNA displayed lower ephrin B1 levels. This suggests that although JunB has a direct effect in cementoblasts to decrease ephrin B1 levels, the effects of reducing JunB levels are modified in different ways by the surrounding environment. It is possible that RNA isolated from the implant reflects other cell types than just the cementoblasts, and highlights the importance of *in vivo* studies to identify operative indirect actions of PTH/PTHrP.

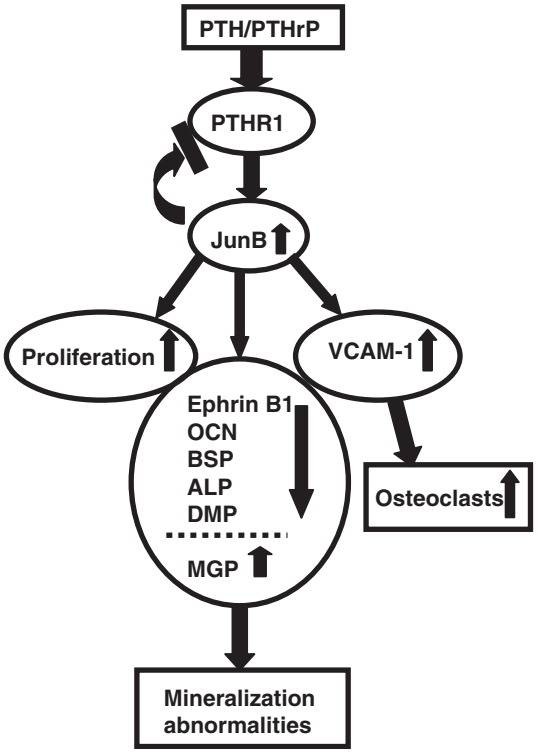

Figure 7 Model of PTHrP actions in cementoblasts. PTH/PTHrP works through its receptor, PTHR1, resulting in an up-regulation of JunB. Feedback to the receptor causes down-regulation of PTHR1, while the increase in JunB initiates downstream effects, including an increase in proliferation, and increase in VCAM-1 (which is known to promote osteoclastic activity), and alterations in many genes involved in mineralization, all of which can lead to perturbations in the normal mineralization process

Our results are summarized in Figure 7: PTH/PTHrP works through its receptor, PTHR1, resulting in an increase in JunB. Feedback to the receptor causes down-regulation, while the increase in JunB initiates downstream effects including an increase in proliferation, an increase in VCAM-1 (which is known to promote osteoclastic activity), and alterations in genes involved in mineralization including ephrin B1, OCN, BSP, alkaline phosphatase, dentin matrix protein, and matrix gla protein, all of which can lead to perturbations in the normal mineralization process. These findings raise new possibilities for the impact of PTHrP on cells in the craniofacial apparatus in the support of osteoclastogenesis and epithelial mesenchymal interactions.

Acknowledgements

Appreciation is extended to Dr Martha Somerman for providing the OCCM cell line and for scientific discussion, to Chris Strayhorn for processing of histological specimens, and

to Andrew Fribley for advice on apoptosis experiments. Disclosure statement: Jan Berry owns stock in Amgen, Eli Lilly and Invitrogen. Laurie McCauley has stock in Amgen and research funding from Eli Lilly unrelated to the presented work. All other authors have no disclosures to report. This study was supported by NIH: DE14073 and DK53904.

Author contributions

Janice E. Berry performed most of the experimental work and prepared the manuscript. Glenda J. Pettway performed the *in vivo* experiments. Kitrina G. Cordell provided histopathological analysis of implants. Taocong Jin performed the microarray analysis and consulted on interpretation of this data. Nabanita S. Datta designed the silencing construct used. Laurie K. McCauley, principal investigator, planned the study, performed data interpretation and prepared the manuscript.

References

Ahmad M, Theofanidis P, Medford RM (1998). Role of activating protein-1 in the regulation of the vascular cell adhesion molecule-1 gene expression by tumor necrosis factor-alpha. *J Biol Chem* **273:** 4616–4621.

Berry JE, Ealba E, Pettway GJ *et al* (2006). JunB as a downstream mediator of PTHrP actions in cementoblasts. *J Bone Miner Res* **21:** 246–257.

Boabaid F, Berry JE, Koh AJ, Somerman MJ, McCauley LK (2004). The role of parathyroid hormone related protein in the regulation of osteoclastogenesis by cementoblasts. *J Periodontol* **75:** 1247–1254.

Brown J (2007). Mouse DNA sequence from cllione RP23-110A15 on chromosome X, complete sequence, Efnb1. *GenBank* **AL671478:** http://www.ncbi.nlm.nih.gov/entrez/viewer.fcgi?db=nuccore&id=21655362.

Calvi LM, Sims NA, Hunzelman JL *et al* (2001). Activated parathyroid hormone/parathyroid hormone-related protein receptor in osteoblastic cells differentially affects cortical and trabecular bone. *J Clin Invest* **107:** 277–286.

Celeste AJ, Rosen V, Bueker JL, Kriz R, Wang EA, Wozney JM (1986). Isolation of the human gene for bone gla proein utilizing mouse and rat cDNA clones. *EMBO J* **5:** 1885–1890.

Chinenov Y, Kerppola TK (2001). Close encounters of many kinds:Fos-Jun interactions that mediate transcription regulatory specificity. *Oncogene* **20:** 2438–2452.

D'Errico JA, Berry JE, Ouyang H, Strayhorn CL, Windle JJ, Somerman MJ (2000). Employing a transgenic animal model to obtain cementoblasts in vitro. *J Periodontol* **71:** 63–72.

Datta NS, Chen C, Berry JE, McCauley LK (2005). PTHrP signaling targets cyclin D1 and induces osteoblastic cell growth arrest. *J Bone Miner Res* **20:** 1051–1064.

Datta NS, Pettway GJ, Chen C-C, Koh AJ, McCauley LK (2007). Cyclin D1 as a target for the proliferative effects of PTH and PTHrP in early osteoblastic cells. *J Bone Miner Res* **22:** 951–964.

Davy A, Soriano P (2005). Ephrin signaling in vivo: look both ways. *Dev Dynam* **232:** 1–10.

Davy A, Aubin J, Soriano P (2004). Ephrin-B1 forward and reverse signaling are required during mouse development. *Gene Dev* **18:** 572–583.

Eferl R, Wagner EF (2005). Fos/AP-1 proteins in bone and the immune system. *Immunol Rev* **208:** 126–140.

Feuerbach D, Feyen JH (1997). Expression of the cell-adhesion molecule VCAM-1 by stromal cells is necessary for osteoclastogenesis. *FEBS Lett* **402:** 21–24.

Fiaschi-Taesch NM, Stewart AF (2003). Minireview: parathyroid hormone-related protein as an intracrine factor-trafficking mechanisms and functional consequences. *Endocrinology* **144:** 407–411.

Gensure RC, Gardella T, Juppner H (2005). Parathyroid hormone and parathyroid hormone-related peptide, and their receptors. *Biochem Biophs Res Commun* **328:** 666–678.

Jin H, Aiyer A, Su J *et al* (2006). A homing mechanism for bone marrow-derived progenitor cell recruitment to the neovasculature. *J Clin Invest* **116:** 652–662.

Jochum W, Passegué E, Wagner EF (2001). AP-1 in mouse development and tumorigenesis. *Oncogene* **20:** 2401–2412.

Kenner L, Hoebertz A, Beil T *et al* (2004). Mice lacking JunB are osteopenic due to cell autonomous osteoblast and osteoclast defects. *J Cell Biol* **164:** 613–623.

Kindle L, Rothe L, Kriss M, Osdoby P, Collin-Osdoby P (2006). Human microvascular endothelial cell activation by IL-1 and TNF-alpha stimulates the adhesion and transendothelial migration of circulating human CD14+ monocytes that develop with RANKL into functional osteoclasts. *J Bone Miner Res* **21:** 193–206.

Koh AJ, Beecher CA, Rosol TJ, McCauley LK (1999). Cyclic AMP activation in osteoblastic cells: effects on PTH-1 receptors and osteoblastic differentiation *in vitro*. *Endocrinology* **140:** 3154–3162.

Kong XF, Schipani E, Lanske B *et al* (1994). The rat, mouse, and human genes encoding the receptor for parathyroid hormone and parathyroid hormone-related peptide are highly homologous. *Biochem Bioph Res Co* **200:** 1290–1299.

Korenaga R, Ando J, Kosaka K, Isshiki M, Takada Y, Kamiya A (1997). Negative transcriptional regulation of the VCAM-1 gene by fluid shear stress in murine endothelial cells. *Am J Physiol – Cell Physiol* **273:** C1506–C1515.

Lee SK, Lorenzo JA (1999). Parathyroid hormone stimulates TRANCE and inhibits osteoprotegerin messenger ribonucleic acid expression in murine bone marrow cultures: correlation with osteoclast-like cell formation. *J Bone Miner Res* **140:** 3552–3561.

Lobb RR, Hemler ME (1994). The pathophysiologic role of alpha 4 integrins in vivo. *J Clin Invest* **94:** 1722–1728.

Lu Q, Sun EE, Klein RS, Flanagan JG (2001). Ephrin-B reverse signaling is mediated by a novel PDZ-RGS protein and selectively inhibits G protein-coupled chemoattraction. *Cell* **105:** 69–79.

Mahon MJ, Donowitz M, Yun CC, Segre GV (2002). Na+/H+ exchanger regulatory factor 2 directs parathyroid hormone 1 receptor signalling. *Nature* **417:** 858–861.

Manen D, Palmer G, Bonjour JP, Rizzoli R (1998). Sequence and activity of parathyroid hormone/parathyroid hormone-related protein receptor promoter region in human osteoblast-like cells. *Gene* **218:** 49–56.

McCabe LR, Kockz M, Lian J, Stein J, Stein G (1995). Selective expression of fos-and jun-related genes during osteoblast proliferation and differentiation. *Exp Cell Res* **218:** 255–262.

Merrill AE, Bochukova EG, Brugger SM *et al* (2006). Cell mixing at a neural crest-mesoderm boundary and deficient ephrin-Eph signaling in the pathogenesis of craniosynostosis. *Hum Mol Genet* **15:** 1319–1328.

Michigami T, Shimizu N, Williams PJ *et al* (2000). Cell-cell contact between marrow stromal cells and myeloma cells via VCAM-1 and alpha(4)beta(1)-integrin enhances production of osteoclast-stimulating activity. *Blood* **96:** 1953–1960.

Niesh AS, Williams AJ, Palmer HJ, Whitley MZ, Collins T (1992). Functional analysis of the human vascular cell adhesion molecule 1 promoter. *J Exp Med* **176:** 1583–1593.

Ogata Y, Nakao S, Kim RH *et al* (2000). Parathyroid hormone regulation of bone sialoprotein (BSP) gene transcription is mediated through a pituitary-specific transcription factor-1 (pit-1) motif in the rat BSP gene promoter. *Matrix Biol* **19:** 395–407.

Pettway GJ, Schneider A, Koh AJ *et al* (2005). Anabolic actions of PTH (1-34): use of a novel tissue engineering model to investigate temporal effects on bone. *Bone* **36:** 959–970.

Pettway GJ, Meganck JA, Koh AJ, Keller ET, Goldstein SA, McCauley LK (2008). Parathyroid hormone mediates bone growth through the regulation of osteoblast proliferation and differentiation. *Bone* **42:** 806–818.

Philbrick WM, Dreyer BE, Nakchbandi IA, Karaplis AC (1998). Parathyroid hormone-related protein is required for tooth eruption. *Proc Natl Acad Sci USA* **95:** 11846–11851.

Priestley GV, Scott LM, Ulyanova T, Papayannopoulou T (2006). Lack of α4 integrin expression in stem cells restricts competitive function and self-renwal activity. *Blood* **107:** 2959–2967.

Saygin NE, Giannobile WV, Somerman MJ (2000). Molecular and cell biology of cementum. *Periodontol 2000* **74:** 73–98.

Schipani E, Kruse K, Jueppner H (1995). A constitutively active mutant PTH/PTHrP receptor in Jansen-type metaphyseal chondrodysplasia. *Science* **268:** 98–100.

Sneddon WB, Syme CA, Bisello A *et al* (2003). Activation-independent parathyroid hormone receptor internalization is regulated by NHERF1 (EBP50). *J Biol Chem* **278:** 43787–43796.

Twigg SR, Kan R, Babbs C *et al* (2004). Mutations of ephrin-B1 (EFNB1), a marker of tissue boundary formation, cause craniofrontonasal syndrome. *Proc Natl Acad Sci USA* **101:** 8652–8657.

Wieacker P, Wieland I (2005). Clinical and genetic aspects of craniofrontonasal syndrome: towards resolving a genetic paradox. *Mol Genet Metab* **86:** 110–116.

Yamashita J, McCauley LK (2006). The activating protein-1 transcriptional complex: essential and multifaceted roles in bone. *Clin Rev Bone Miner Metab*. **4:** 107–122.

Yang R, Gerstenfeld LC (1996). Signal transduction pathways mediating parathyroid hormone stimulation of bone sialoprotein gene expression in osteoblasts. *J Biol Chem* **274:** 29839–29846.

Young MF, Ibaraki K, Kerr JM, Lyu MS, Kozak CA (1994). Murine bone sialoprotein (BSP): cDNA cloning, mRNA expression, and genetic mapping. *Mamm Genome* **5:** 108–111.

Zhao C, Irie N, Takada K *et al* (2006). Bidirectional ephrinB2-EphB4 signaling controls bone homeostasis. *Cell Metab* **4:** 111–121.

Zhou H, Zarubin T, Ji Z *et al* (2005). Frequency and distribution of AP-1 sites in the human genome. *DNA Res* **12:** 139–150.

Supporting information

Additional supporting information may be found in the online version of this article.

In vitro Array, genes down 2X or more, PTHrP and JunB paper.

In vitro Array, genes up 2X or more, PTHrP and JunB paper.

Genes down-regulated both *in vitro* and *in vivo*, PTHrP and JunB paper.

Genes up-regulated both *in vitro* and *in vivo*, PTHrP and JunB paper.

In vivo Array, genes down 2X or more, PTHrP and JunB paper.

In vivo Array, genes up 2X or more, PTHrP and JunB paper.

Please note: Wiley-Blackwell are not responsible for the content or functionality of any supporting information supplied by the authors. Any queries (other than missing material) should be directed to the corresponding author for the article.